ARMA 18–363

A Case Study of Pillar Collapse at a Limestone Mine in Pennsylvania

Esterhuizen G.S.
NIOSH Pittsburgh Mining Research Division, Pittsburgh, PA, USA
Tyrna, P.L.
MSHA Technical Support Group, Triadelphia, VW, USA
Murphy, M.M.
NIOSH Pittsburgh Mining Research Division, Pittsburgh, PA, USA

This paper was prepared for presentation at the 52nd US Rock Mechanics / Geomechanics Symposium held in Seattle, Washington, USA, 17–20 June 2018. This paper was selected for presentation at the symposium by an ARMA Technical Program Committee based on a technical and critical review of the paper by a minimum of two technical reviewers. The material, as presented, does not necessarily reflect any position of ARMA, its officers, or members. Electronic reproduction, distribution, or storage of any part of this paper for commercial purposes without the written consent of ARMA is prohibited. Permission to reproduce in print is restricted to an abstract of not more than 200 words; illustrations may not be copied. The abstract must contain conspicuous acknowledgement of where and by whom the paper was presented.

ABSTRACT: The sudden collapse of approximately 3 Ha of room-and-pillar workings at a limestone mine in southwestern Pennsylvania in 2015 resulted in an air-blast that injured three mine workers. Subsequent investigations showed that an area encompassing 35 pillars had collapsed. The pillars were 9 to 10 m wide and up to 18 m high. A notable geologic feature is the through-going joints that dip at 50° to 80° and can extend from the roof to the floor of the pillars. These structures are thought to have weakened the pillars well below the strength that is predicted by empirical equations for hard-rock pillar design. This paper presents the relevant geotechnical data related to the collapsed area and numerical model results that were used to estimate the pillar loading underneath the variable topography and compares the pillar loads to some established hard-rock pillar strength equations. The outcome is also compared to a strength equation that was developed specifically for limestone mines in which the negative impact of large angular discontinuities is explicitly accounted for. The results show that the critical state of the workings would have been predicted correctly by the limestone pillar strength equation.

1. INTRODUCTION

On April 29, 2015 three miners were waiting near the portal of an underground limestone mine in southwestern Pennsylvania when they heard something like shots being fired in the mine. This was followed by a massive collapse of the room-and-pillar workings in the mine. The air-blast from the collapse knocked the miners to the ground, causing serious injuries to each miner. Subsequent investigations revealed that subsidence of the mountainside overlying the mine workings had occurred. The subsidence area encompassed about 3 Ha. Underground inspections to delineate the collapsed area showed that about 35 pillars had collapsed. A wide-angle, aerial camera view of the mine showing the main portal and the subsidence area is presented in Figure 1.

The objective of this paper is to describe the geotechnical and mining factors associated with the pillar failure and to demonstrate how large through-going discontinuities reduced the pillar strength well below the strength that would have been predicted by established hard-rock pillar strength equations. An equation that accounts for the impact of such large discontinuities is presented, and it is shown that this equation would have identified the critical stability of the pillars at the case study mine.

2. GEOTECHNICAL PARAMETERS

2.1. Geologic setting

The mine is located in the Appalachian Plateau and is situated 120 meters beneath the crest of Chestnut Ridge in southwestern Pennsylvania, U.S.A. Chestnut Ridge is a northeast trending, roughly 150 kilometers long, doubly plunging anticline with a maximum topographical relief of 300 meters. It is asymmetrical, with steeper dipping strata on the northwest side. This ridge represents the western edge of the Allegheny Mountains and the western extent of fold structures associated with the Appalachian orogeny.

The Loyalhanna limestone extracted at the mine typically occurs at depth in the region, but is mined in numerous locations where folding has brought it nearer to the surface. Underground, the folding is hardly noticeable because the collapsed mine workings occur near the fold hinge. In southwestern Pennsylvania, the Loyalhanna is stratigraphically a lower member of the 1,000 to 1,500-meters thick, Mississippian-age Mauch Chunk Formation. The Loyalhanna limestone has a maximum

thickness of 30 meters, but is typically 20 meters thick in the Chestnut Ridge mines. It is light to greenish-gray and compositionally ranges from a calcareous sandstone to a sandy limestone. At the mine, the Loyalhanna limestone bed is overlain by distinctive reddish-brown mudstones, shales, and siltstones of the Mauch Chunk beds, shown in Figure 2.

Figure 1. Aerial view of the mine showing extent of surface subsidence associated with the collapse of the pillars.

Figure 2. Main portal entering the mine with Mauch Chunk beds exposed in the highwall.

2.2. Geologic Structure

Geologic features typically associated with Appalachian fold structures, including thrust faults and transverse, conjugate, and longitudinal joints, were present in the mine. A well-defined thrust fault was visible in the highwall immediately north of the Haulage (south) Portal. The N25°E striking fault was planar with approximately 1.5 meters of apparent offset. Dip was calculated at 15 degrees southeast. The fault intersected the top of the mining horizon near the south portal and intersected the surface along the southeast edge of the pillar collapse subsidence trough. Within the mining horizon, the fault was coincident with ground control mitigation features, including a steel canopy in the main roadway and larger, non-uniform pillars in older mine workings. Degraded ground conditions associated with the fault were more pronounced in the eastern portion of the mine. The strike of the fault was approximately parallel with the axis of the Chestnut Ridge anticline and other fault structures described in previous studies (Iannacchione and Coyle, 2002).

Jointing observed underground showed multiple orientations, although most joints fell generally into a northwest and northeast set with dips ranging from vertical to less than 30°. One particular set of joints stood out in terms of prominence, persistence, and uniformity. This set, with a strike of N60°W, occurred in a well-defined zone 150 meters wide that intersected the main portal area and the eastern half of the pillar collapse zone. Joints in the zone were typically spaced 3-5 m apart and dipped 60° to 80° to the southwest, shown in Figure 3. Some joint traces exposed by the pillars were curvilinear with dips less than 60° in the lower portion of the pillar. Many of the joints near the collapsed area were dilated by groundwater dissolution and some showed apertures up to 6 inches. The joints were perpendicular to the northeast striking thrust fault and are interpreted as transverse joints associated with anticline formation.

Figure 3. Prominent N60°W striking joint intersecting a pillar south of the collapsed area.

2.3. Rock Strength and Rock Mass Classification

Rock strength testing and rock mass classification of the Loyalhanna limestone at this mine was conducted by the National Institute of Occupational Safety and Health (Esterhuizen et al. 2006) as part of a survey of pillar

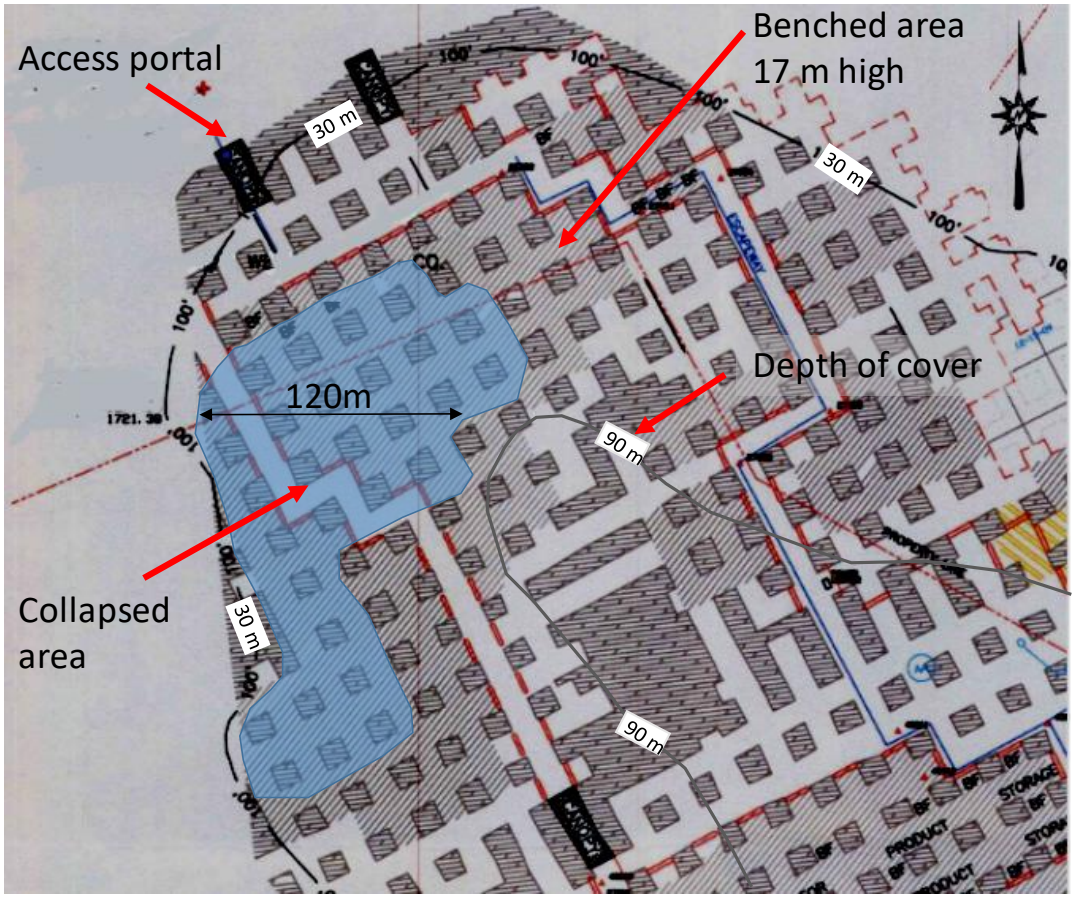

Figure 4. Portion of the mine map showing the room-and-pillar workings and the collapsed area.

design practices in limestone mines. The rock mass was classified at three locations using the Bieniawski (1989) Rock Mass Rating (RMR). The ratings were found to range from 69 to 76, placing the rock mass slightly below the average RMR of 75 found in the survey of limestone mines.

Rock samples were collected from the operational area of the mine, and five of these samples were tested providing an average uniaxial compressive strength (UCS) of 182 MPa, which is somewhat lower than expected for the Loyalhanna limestone, which is usually in the range of 200 to 220 MPa. However, the lower rock strength is consistent with the strength testing results determined during the initial mining permit application for the mine (Smith, 2016)

3. MINING PLAN

3.1. Mining layout and original pillar design

The initial mining plan in the mining permit called for a room-and-pillar layout with 10.7-m x 10.7-m square pillars and rooms that are 13.7 m wide. The mining was planned to be conducted in two lifts, first mining the upper 7.0 m and followed by bench mining between the pillars to increase the mining height to 16.1 m. The layout is thought to be largely driven by mining practices at other mines in the area. The designed pillars, therefore, would have width-to-height ratios of 0.66. The maximum depth of cover under the mountain that overlies the limestone body is 120 m. In the collapse area, the depth of cover ranges from about 30 m to 90 m.

Figure 4 shows the mining layout and the outline of the area that collapsed. A relatively regular pillar layout was followed starting at the portals, but as the mine progressed, poor ground conditions were encountered near the low-angle fault exposed in the highwall and underground. As a result, large blocks of ground were left intact with the objective to resume mining beyond the poor ground. During this time, bench mining was conducted in the area near the portals. Bench mining more than doubled the height of the pillars, exposing continuous angular joints that caused sections of the intended pillars to fall away during the blast. Figure 5 shows such a pillar observed around the year 2001 (Iannacchione, 2016).

In subsequent years, portions of the benched area were backfilled with fine crusher waste that may have provided some confinement to the lower half of the pillars. The backfilling did not extend above the mid-height of the benched pillars. The area that collapsed had not been actively mined for approximately 15 years when the collapse occurred. Over the life of the mine a secondary escapeway had at times passed through the event area.

4. OBSERVATIONS AROUND THE PERIMETER OF THE COLLAPSED AREA

During the inspection mine visit, it was possible to enter the mine through the portal at the northern extent of the mine, right next to the collapsed area. The mine escapeway was open, and it was possible to travel along the northern limit of the collapse and around to the southern extent of the collapse. It appeared that the backfilling material may have prevented some of the benched pillars adjacent to the collapsed area from failing. The exact extent of backfilling was unknown.

Figure 5. A pillar impacted by large angular joints along the edge of bench mining (photo, by A.T. Iannacchione).

Figure 6. Pillar adjacent to collapsed area affected by angular jointing.

4.1. Measured pillar dimensions

During an inspection of the collapsed area in August 2016 measurements were made of the actual pillar dimensions around the perimeter of the collapsed area. It was found that the average pillar width was 9.5 m with a standard deviation of 1.3 m. The average room width was 14.5 with a standard deviation of 0.6 m. It was not possible to measure the full height of the pillars at the collapsed area, however, in adjacent stable areas,

Figure 7. Rubble from the roof collapse and a stable pillar along the edge of the benched area that collapsed.

measurements showed the mining height to be 17.7 m. The average width-to-height ratio is therefore 0.54 with 84% extraction ratio in the room-and-pillar panels.

Figure 6 shows a pillar along the escapeway, which demonstrated the type of roof-to-floor jointing observed in this part of the mine. Note that the walkway was not bench mined and was, therefore, about 10 m above the floor of the benched area.

Figure 7 shows the roof rubble that flowed between the pillars during the collapse. None of the collapsed pillars were visible, owing to the volume of roof rubble that flowed into the mine voids. This raised the question of whether it may have simply been a roof collapse. However, the significant depth of subsidence, without signs of pillar humps on the surface, and the abruptness of the collapse rules out that the pillars may still be standing in the collapsed area. A roof collapse would be expected to be more progressive, taking place over an extended period of time.

5. ANALYSIS OF PILLAR LOADING

Back analysis of the pillar strength in a collapsed panel is usually based on the assumption that, at the time of collapse, the pillar strength was equal to the imposed

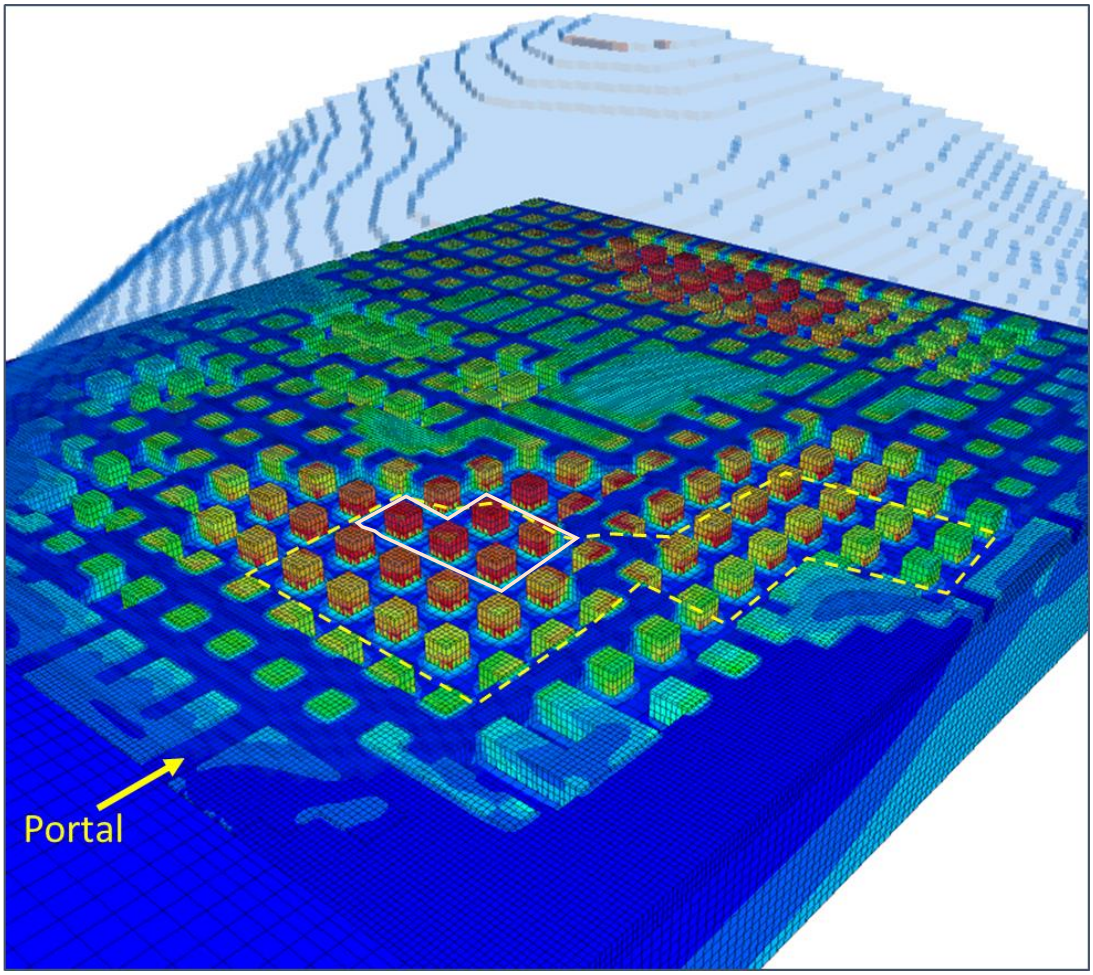

Figure 8. Numerical model of the mine and overlying mountain colored by the vertical stress magnitude. The collapsed area is outlined with dashed lines, and the cluster of pillars with the highest average stress is outlined with a solid line.

overburden load. In this case, the overburden depth varies from about 30 m to 90 m, which complicates the calculation of the overburden loading. Also, the overburden load will vary significantly based on the depth. Consequently the FLAC3D finite difference program (Itasca, 2014) was used to create a model of the mountain and the mine workings within the mountain.

5.1. Model setup

The model material was assumed to be elastic so that the pre-failure stress distribution could be determined. The mined-out region was discretized with sufficient detail to simulate the pillars and benched areas. The element width for modeling the mined zone was selected as 2.0 m, allowing each pillar to be modelled with five elements across its width. Pillars were modelled to be 10.0 m wide, and the rooms were modelled to be 14.0 m wide. The overlying strata was modelled using 3-m-wide elements. The immediate roof of the mined workings consisted of about 2 m of limestone left intact to prevent breakthrough to the weaker overlying Mauch Chunk strata. This stiffer roof layer was included in the model. Figure 8 shows a cutaway view of the model in which the pillars were horizontally sliced at mid-height and the mountain is shown as a transparent overlay. Since the mine workings were essentially above the valley floor, no horizontal stress was initialized in the model. The boundary conditions along the sides of the model were set to restrict horizontal displacement only while the bottom surface was fixed in the vertical direction. The model loading was purely by gravity. The model included the "nose" of the mountain, the collapsed workings, and a portion of the mine beyond the collapsed area. The coloring of the model shown in Figure 8 depicts the resulting vertical stress distribution in the pillars and surroundings.

5.2. Pillar loading results

The FLAC3D-calculated vertical stress at mid-height of the pillars was used to calculate the average stress in each pillar. The average pillar stress of the individual pillars within the collapsed area varied from the maximum of 11.7 MPa down to 5.3 MPa for the pillars under the shallowest cover. A simple tributary area pillar stress calculation, based on a depth of cover of 90 m and 84% extraction, results in an average predicted pillar stress of 13.3 MPa. This slightly higher stress is expected because it assumes a flat ground surface, while the FLAC3D model accurately models the effect of the sloping topography.

The model stress results showed that there was a cluster of five pillars near the edge of the collapsed area, under the ridge of the mountain that had the greatest vertical stress. The calculated average vertical stress in each of these pillars varied from 10.0 to 11.7 MPa, with an average value of 11.0 MPa for the five pillars combined. It was assumed that the collapse initiated when one or more of these pillars failed.

6. ANALYSIS OF PILLAR STRENGTH

For the purpose of further analysis, it is assumed that the 11.0-MPa stress in the cluster of five pillars represents the strength of the pillars at the time of the collapse. This pillar strength is only 6% of the intact rock strength tested in the laboratory.

6.1. Comparison to empirical hard-rock pillar strength equations

The calculated pillar strength at the case study mine was compared to the strength that would be predicted by some of the widely used empirical hard-rock pillar strength equations. The selected equations are the Hedley and Grant (1972) equation:

$$S = k\frac{w^{0.5}}{h^{0.75}} \qquad (1)$$

The Krauland and Soder (1987) equation for limestone:

$$S = k(0.778 + 0.222\left(\frac{w}{h}\right)) \qquad (2)$$

The Lunder and Pakalnis (1997) equation:

$$S = 0.44\sigma_c(0.68 + 0.52\kappa) \qquad (3)$$

where k is the large-scale rock strength, w is the pillar width, h is the pillar height, σ_c is the intact rock strength, and κ is a confinement parameter. The pillar strengths for 17.7-m-high pillars of various widths were calculated using each equation and shown in Figure 9. For the Hedley and Grant equation, the strength factor relating the large-scale rock strength to the laboratory-scale UCS is 0.58, and for the Krauland and Soder equation the strength factor is 0.354. The actual pillar strength from this case study is also shown in Figure 9. It is clear that the empirically based strength equations would have grossly overestimated the actual pillar strength and would have predicted stable conditions at the mine.

The reason for the discrepancy between the empirical equations and the actual pillar strength at the case study mine is clearly the presence of large angular discontinuities cutting through the slender pillars. It appears that the case studies that were used to develop the empirical equations did not include any cases of such slender pillars with large through-going discontinuities.

6.2. Accounting for large discontinuities

The potential importance of large through-going discontinuities on the strength of slender pillars was recognized during the NIOSH research into U.S. limestone mine pillar strength (Esterhuizen et al. 2006; Esterhuizen et al. 2011). Large through-going discontinuities are loosely defined as discontinuities that have dip trace lengths greater than 50% of the pillar height and may daylight on opposite sides of a pillar.

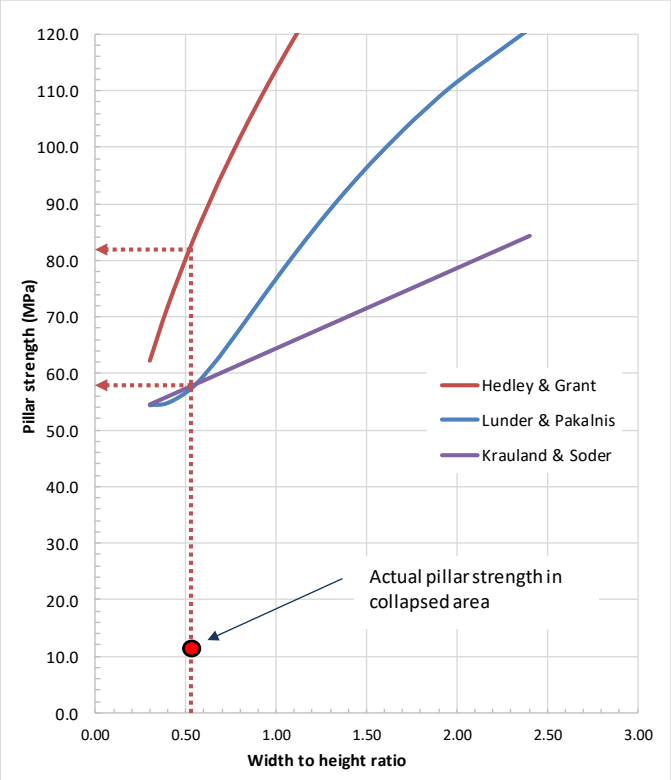

Figure 9. Actual pillar strength at the case study mine compared to predictions using established hard-rock pillar strength equations.

During this research, several single pillar failures associated with large through-going discontinuities were observed in otherwise stable workings, but no wide area collapses had occurred that would allow back analysis of average pillar loading and average pillar strength. Simple two-dimensional models of pillars were, therefore, used to investigate the potential impact of large through-going discontinuities on pillar strength. The UDEC (Itasca, 2006) discrete element stress analysis software was used to simulate numerous pillar and discontinuity configurations. The model input parameters were selected to correctly simulate case histories of pillars with large through-going discontinuities that had not failed.

It was found that the impact of such large through-going discontinuities diminished as the pillar width-to-height ratio increased. Tall, slender pillars were shown to be significantly impacted, while wider pillars at width-to-height ratios exceeding 1.2 showed reduced impact. Discontinuity dips of around 60° were found to have the most significant impact on pillar strength.

Table 1. The discontinuity dip factor (DDF) representing the strength reduction caused by a single discontinuity intersecting a pillar at or near its center, used in Equation 5.

	Pillar width-to-height ratio								
Dip (°)	≤0.5	0.6	0.7	0.8	0.9	1.0	1.1	1.2	>1.2
30	0.15	0.15	0.15	0.15	0.16	0.16	0.16	0.16	0.16
40	0.23	0.26	0.27	0.27	0.25	0.24	0.23	0.23	0.22
50	0.61	0.65	0.61	0.53	0.44	0.37	0.33	0.30	0.28
60	0.94	0.86	0.72	0.56	0.43	0.34	0.29	0.26	0.24
70	0.83	0.68	0.52	0.39	0.30	0.24	0.21	0.20	0.18
80	0.53	0.41	0.31	0.25	0.20	0.18	0.17	0.16	0.16
90	0.31	0.25	0.21	0.18	0.17	0.16	0.16	0.15	0.15

Table 2. The frequency factor (FF) used in Equation 5 to account for the spacing of large discontinuities.

Average frequency of large discontinuities per pillar	Frequency factor (FF)
0.0	0.00
0.1	0.10
0.2	0.18
0.3	0.26
0.5	0.39
1.0	0.63
2.0	0.86
3.0	0.95
>3.0	1.00

A strength equation for square limestone pillars was developed based on the findings of Roberts et al. (2007) in the Missouri lead belt mines. The impact of large discontinuities was introduced as an additional parameter that accounts for the frequency and inclination of any large through-going discontinuities.

The final equation developed for estimating limestone mine pillar strength is as follows (Esterhuizen et al. 2011):

$$S = 0.65 \times UCS \times LDF \times \frac{w^{0.30}}{h^{0.59}} \qquad (4)$$

where *UCS* is the uniaxial compressive strength of the intact rock, *LDF* is a factor to account for the presence of large discontinuities, *w* and *h* are the pillar width and height in meters. The large discontinuity factor accounts for the dip and frequency of the discontinuities:

$$LDF = 1 - DDF \times FF \qquad (5)$$

where *DDF* is the discontinuity dip factor shown in Table 1, and *FF* is the frequency factor related to the frequency of large discontinuities per pillar shown in Table 2.

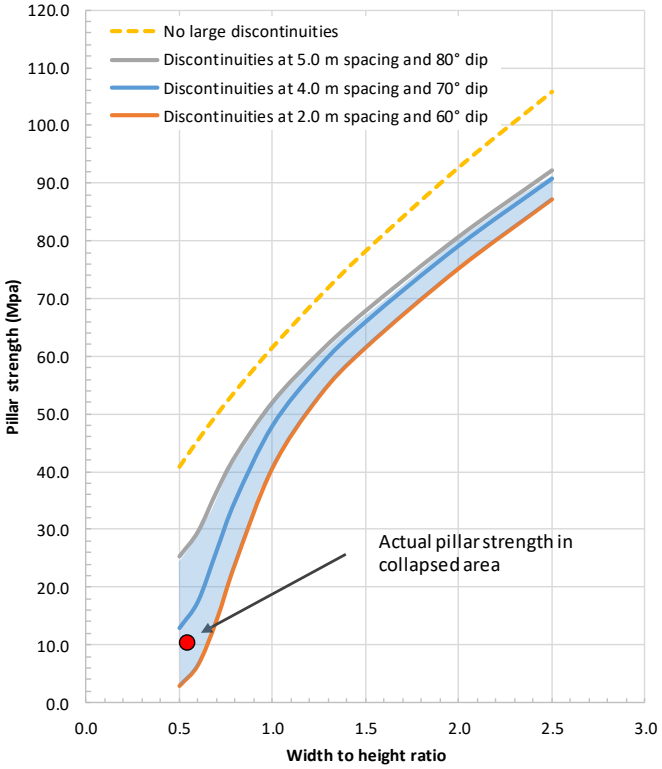

Figure 10. A graphs showing range of pillar strengths determined for the 17.7-m-high collapsed pillars using Equations 4 and 5.

The strength of the pillars at the case-study mine was calculated using Equations 4 and 5. Inputs were as follows:

UCS of intact rock = 182 MPa
Dip of large discontinuities = 50°-80°
Spacing of large discontinuities = 2 to 5 m
Pillar width = 9.5 m
Pillar height = 17.7 m

The range of pillar strength results obtained using Equations 4 and 5 are shown in Figure 10. The figure also shows the predicted pillar strength in the absence of any large discontinuities. The range of strengths was determined by varying only the large discontinuity

spacing and dip. The minimum strength is actually achieved when the discontinuity dip is 60°, which was selected to derive the minimum strength curve. The upper solid curve is obtained by selecting the maximum discontinuity spacing of 5.0 m and a dip of 80°.

The results show that the equation predicts a significant drop in pillar strength at the lower width-to-height ratios. Also, the range of likely strengths based on the variability of the large discontinuity geometry includes the actual pillar strength. If the average dip and spacing of the most prominent joint set is used, at 70° and 4.0 m respectively, the equation predicts a pillar strength of 12.9 MPa.

The results show that accounting for the impact of large through-going discontinuities would have provided a clear indication of the critical stability condition of the pillars at the case study mine.

6.3. Alternative approaches to account for discontinuities

More recently, the impact of discrete discontinuities on pillar strength and the need to account for the large-scale rock mass strength on pillar strength has received increased attention. For example, Elmo and Stead (2010) have used discrete element models to investigate rock mass characteristics and discrete joints on pillar strength, while Oke and Esterhuizen (2017) used a more pragmatic approach to account for both rock mass strength and the impact of discontinuity dip. These approaches are likely to further contribute to improved estimates of pillar strength, especially in the low width-to-height ratio ranges encountered in shallow underground room-and-pillar mines.

7. CONCLUSIONS

A case study has been presented in which tall, slender pillars collapsed causing an air-blast at a limestone mine in southwestern Pennsylvania. The pillars were about 17 m tall and 9.5 m wide. The collapsed pillars were evaluated using a three-dimensional numerical model to estimate the loading on the pillars. Using these results, it was demonstrated that widely used pillar strength equations for hard rock mines would have significantly over-estimated the strength of the collapsed pillars. It was concluded that large angular discontinuities within the pillars contributed to the collapse. A pillar strength equation with a parameter to account for the presence of such through-going discontinuities was shown to be able to accurately capture the reduced strength of the pillars. Pillar design engineers need to be aware of the potential to over-estimate the strength of slender pillars that are affected by large angular discontinuities.

8. REFERENCES

Bieniawski, Z.T., 1989. *Engineering rock mass classifications*. New York: Wiley.

Elmo, D. and D. Stead. 2010. An integrated numerical modelling discrete fracture network approach applied to the characterization of rock mass strength of naturally fractured pillars. Rock Mechanics and Rock Engineering 43, 3–19.

Esterhuizen, G.S., A.T. Iannacchione, J.L Ellenberger, and D.R. Dolinar. 2006. Pillar stability issues based on a survey of pillar performance in underground limestone mines. In *25th International Conference on Ground Control in Mining*, Morgantown, WV, pp. 354–361.

Esterhuizen, G.S. and D.R. Dolinar, J.L. Ellenberger J.L. 2011. Pillar strength in underground stone mines in the United States. *Int J Rock Mech Min Sci* 2011 Jan; 48(1):42–50.

Hedley, D.G.F. and F. Grant. 1972. Stope-and-pillar design for the Elliot Lake Uranium Mines. *Bulletin of Canadian Institute of Mining and Metallurgy* 65, 37–44.

Iannacchione, A.T. and P.R. Coyle. 2002. An examination of the Loyalhanna limestone's structural features and their impact on mining and ground control practices. In *21st International Conference on Ground Control in Mining, August 6-8, 2002*, Morgantown, West Virginia. Peng SS, Mark C, Khair AW, Heasley KA, eds., 218–227. Morgantown, WV.

Iannacchione, A.T. 2016. University of Pittsburgh, Personal communication, Pittsburgh, PA, 2016.

Itasca Consulting Group. 2006. Software: Universal Distinct Element Code (UDEC), Minneapolis, 2006.

Itasca Consulting Group. 2014. Software Fast Lagrangian Analysis of Continua in 3 Dimensions (FLAC3D), Minneapolis, 2014.

Krauland, N. and P.E. Soder. 1987. Determining pillar strength from pillar failure observations. *Engineering and Mining Journal* 8, 34–40.

Lunder, P.J. and R. Pakalnis. 1997. Determination of the strength of hard- rock mine pillars. *Bulletin of Canadian Institute of Mining and Metallurgy* 90, 51–55.

Oke, J. and G.S. Esterhuizen. 2017. Improving hard rock pillar design by including rock mass classification and failure mechanisms. In *51st US Rock Mechanics/Geomechanics Symposium*, San Francisco, California, 25–28 June.

Roberts, D., D. Tolfree, and H. McIntyre. 2007. Using confinement as a means to estimate pillar strength in a room and pillar mine. In: E. Eberhardt, D. Stead, T. Morrison, editors. *Proceedings of the first Can-US rock mechanics symposium*. London: Taylor & Francis, 2007. p. 1455–61.

Smith, G. 2016. Pennsylvania Department of Environmental Protection, Personal communication, Pittsburgh, PA.